

3C 279 multiwavelength observation in the *Fermi* era

Masaaki Hayashida*, Greg Madejski* and Werner Collmar† for the *Fermi*-LAT collaboration

*Kavli Institute for Particle Astrophysics and Cosmology, SLAC National Accelerator Laboratory, CA, 94025, USA

†Max-Planck Institut für extraterrestrische Physik, 85748 Garching, Germany

Abstract. The Flat Spectrum Radio Quasar 3C 279 ($z = 0.536$), the first γ -ray blazar discovered by EGRET, was one of the brightest γ -ray sources in the sky at the time of its discovery. The LAT detector on board the *Fermi* Gamma-ray Space Telescope has detected significant γ -ray emission from the source. Thanks to the much higher sensitivity and wider field-of-view than ones of EGRET, *Fermi*-LAT is uninterruptedly monitoring the source with an unprecedented accuracy in the gamma-ray band. The γ -ray flux shows strong variability. The integrated flux above 200 MeV varied in the range from 1 up to 9×10^{-7} photons $\text{cm}^{-2} \text{s}^{-1}$ during the first 7-month observation. We have organized intensive multiwavelength campaigns of 3C 279 in a wide-energy range from radio to TeV energy bands during the first *Fermi* year. In this paper, we report the first results of 3C 279 from *Fermi* as a part of the multiwavelength observations.

Keywords: *Fermi*-LAT blazar 3C 279

I. INTRODUCTION

Blazars are Active Galactic Nuclei (AGN) characterized by highly luminous and rapidly variable continuum emission at all observed bands. In 1990s, the EGRET instrument on board *Compton Gamma-Ray Observatory* (CGRO) has revealed that blazars are the dominant class of γ -ray emitters in the extra-galactic sky [12]. 3C 279 ($z = 0.536$) is one of the first γ -ray blazars discovered by EGRET in 1991 [11]. The γ -ray signal had been persistently detected in each observation by EGRET since its discovery. The γ -ray flux varied by roughly 2 orders of magnitude in the range from $\sim 10^{-7}$ up to $\sim 10^{-5}$ photons $\text{cm}^{-2} \text{s}^{-1}$ above 100 MeV [16], [24], and has displayed a factor of 2 variation on a timescale as short as 8 hr. The photon index in the EGRET γ -ray band ranged from 1.8 to 2.3 [20]. Those authors also searched for a possible trend of spectral hardening with the increased flux, but no clear evidence was found.

3C 279 was also detected at lower energies by CGRO's OSSE (50 keV – 1 MeV) [18] and COMPTEL (0.75–30 MeV) [14], [6].

In July 2006, the AGILE satellite observed a γ -ray flare associated with the source with 11.1σ significance [9]. They reported an average flux above 100 MeV of $(21.0 \pm 3.8) \times 10^{-7}$ photons $\text{cm}^{-2} \text{s}^{-1}$ with the photon index of 2.22 ± 0.23 between 100 and 1000 MeV

Recently, the imaging atmospheric Cherenkov telescope MAGIC detected a very-high-energy (VHE) γ -ray flare above 80 GeV [1], which made this source the most distant known VHE γ -ray emitter.

The broad band spectral energy distribution (SED) of the source is characterized by a two-bump structure. The first one, peaking at the far-IR, is commonly ascribed to synchrotron radiation from relativistic electrons in the jet while the second bump, ranging from the X-ray to the γ -ray band with a peak in the MeV-GeV range, is believed to be generated via inverse-Compton scattering. In such so-called "leptonic model", the seed photons can be the synchrotron photons (synchrotron self-Compton: SSC [15], [4]), accretion disk photons (external Compton scattering of direct disk radiation: ECD [7], [8]) and accretion disk photons re-scattered by the broad-line region (external Compton scattering of radiation reprocessed by broad line region clouds/intercloud medium: ECC [21], [3]).

As those sources show strong variability in most accessible energy bands, simultaneous multiwavelength observations over a wide energy range are essential to study the physics of these high-energy radiation emitters. Multiwavelength snapshot observations for several epochs were presented in [13]. They explained their SEDs using the leptonic model; X-ray photons are mainly produced by SSC, and both ECD and ECC are likely to contribute to the γ -ray emission. Spectral variability is consistent with variations of the bulk Lorentz factor of the jet, accompanied by changes in the spectral shape of the electron distribution. On the other hand, since radiation in different spectral bands does not always rise and fall simultaneously, multi-band monitoring observations are particularly important to understand the variability patterns in various energy bands. For example, [5] present results of multi-band monitoring for 11 years in radio, optical and X-ray and discuss the details of the jet structure based on multi-band correlation studies. However, due to the lack of instruments, long term monitoring observations could not include the γ -ray band, in which the source often shows stronger variability than in other bands.

The *Fermi* Gamma-ray Space Telescope was successfully launched on June 11, 2008. The LAT [2] instrument on *Fermi* covers a simultaneous field of view of 2.4 steradians on the sky. Compared to earlier γ -ray missions, the LAT has a larger effective area (8,000 cm^2 on axis at 1 GeV for the event class considered

here), and a wider energy coverage, from 20 MeV to > 300 GeV. During the first year of operations, most of the telescope's time is being dedicated to the "survey mode." In the survey mode, the instrument z-axis is offset 35° North and South from the spacecraft zenith during alternate orbits in order to provide complete sky coverage every three hours. Therefore, *Fermi*-LAT uninterruptedly monitors all γ -ray sources on the sky with an unprecedented accuracy.

Taking advantage of this new instrument for γ -ray observations, we have organized planned intensive multi-wavelength campaigns for 3C 279 from radio to the TeV energy range during the first *Fermi* year. Many ground-based telescopes (cm, mm, near IR-optical and VHE γ -ray) and various satellites (*Suzaku*, *XMM-Newton*, *INTEGRAL*, *RXTE/PCA*, *Swift* and *Spitzer*) participate in such campaigns. In this paper, we report the first results of 3C 279 from *Fermi* as a part of the multiwavelength observations. More extensive studies including other multiwavelength data and detailed discussions of emission models will be presented in forthcoming papers.

II. OBSERVATIONS AND DATA ANALYSIS

The data used here comprise 7-month observations obtained between August 4, 2008 and March 11, 2009 (54682 - 54901 MJD), corresponding to the interval runs from 239500800 to 258422400 MET (Mission elapsed time). We used the most recent version of the standard LAT analysis software, *ScienceTools v9r11*. The events were selected using the most stringent set of standard analysis cuts and correspond to the so-called "diffuse class" events. In addition, we excluded the events with zenith angles greater than 105° to avoid the contamination of the Earth's bright γ -ray albedo. The events were extracted in the range 200 MeV-300 GeV and within a 17° acceptance cone of the Region of Interest (ROI) centered on the location of 3C 279 (RA = 195.047°, DEC=-5.789°, J2000). Below 200 MeV, the collection area of LAT for the diffuse class events drops very quickly and thus larger systematics are expected. Gamma-ray flux and spectrum were calculated using the instrument response function of "P6_V3_DIFFUSE" by an unbinned maximum likelihood fit of model parameters. The source model in our analysis includes point sources for 3C 279 and three other bright sources inside the ROI: 3C 273, PKS 1329-049 and 0FGLJ1231.5-1410. Besides, the model also includes a component for the Galactic diffuse emission along the plane of the Milky Way derived using the GALPROP code [22] and an isotropic power-law component to represent the extragalactic diffuse emission and some residual instrumental background. We examine the significance of the γ -ray signal from those sources by means of the test statistics (TS) based on the likelihood ratio test [17].

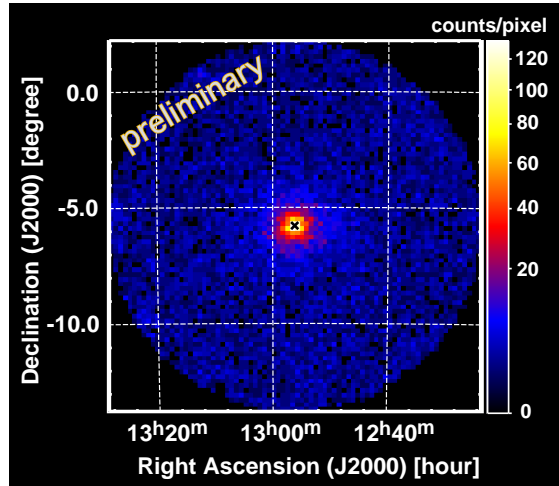


Fig. 1: Sky map of γ -ray events centered on 3C 279 (image radius of 8°) above 200 MeV as measured by *Fermi*-LAT. The nominal position of 3C 279 is marked by cross. The pixel size corresponds to $0.2^\circ \times 0.2^\circ$.

III. RESULTS

A. Skymap

Figure 1 shows the *Fermi*-LAT raw count map of γ -ray events (diffuse class) above 200 MeV centered on the position of 3C 279 with an image radius of 8°. The pixel size corresponds to $0.2^\circ \times 0.2^\circ$. Above 200 MeV, more than 4000 γ -ray photons associated with 3C 279 were detected during the 7-month observations.

B. Light curve

Figure 2 presents the γ -ray light curve during the 7-month observation, where the integrated flux above 200 MeV ($F_{E>200\text{MeV}}$) is plotted as measured by *Fermi*-LAT. Each point is the flux averaged over 3 days. The light curve consists of 73 points, among which 67 points have TS > 25 and only one point (20th point: 54740 MJD) has TS < 9 for the γ -ray signal.

The γ -ray flux clearly shows variability. At the beginning of the observations, the source exhibited a low state of activity with $F_{E>200\text{MeV}} \sim 1\text{-}2 \times 10^{-7}$ photons $\text{cm}^{-2} \text{s}^{-1}$. In November 2008, the flux increased and reached the maximum of $F_{E>200\text{MeV}} \sim 9 \times 10^{-7}$ photons $\text{cm}^{-2} \text{s}^{-1}$ at the end of November 2008 (~ 54800 MJD) with the measured rise/fall flux-doubling times of ~ 5 days. The source keeps a rather high state until the end of the 7-month period covered here. In this paper, we define the period after November 11, 2009 (54779 MJD) as the "active period".

In Figure 3, the flux in the 200-800 MeV band (soft band) is plotted against the flux above 800 MeV (hard band). The fluxes were averages in a 3-day interval. Only data points with TS > 16 for the γ -ray signal in the each band are used for the plot. We fitted the flux-flux plot with a linear function. The plot is well described by the linear function between the soft and hard bands with a slope of 0.25 ± 0.02 and a small

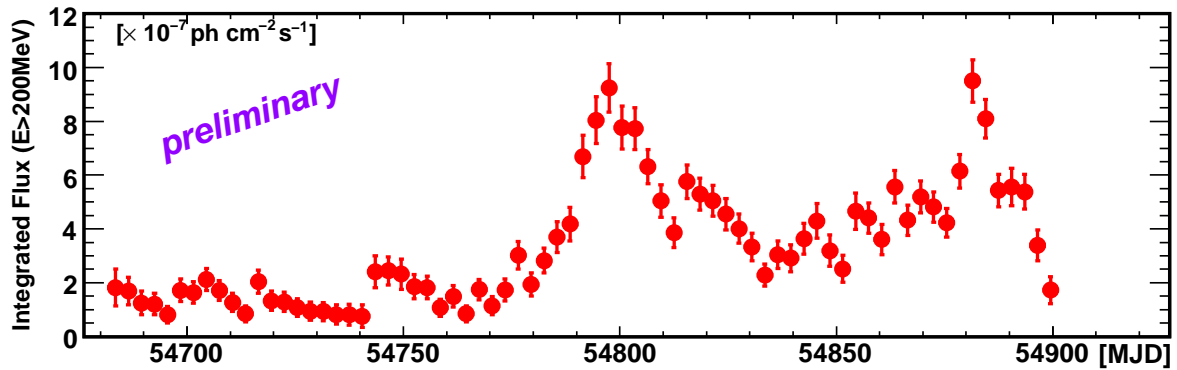


Fig. 2: Gamma-ray light curve of 3C 279 above 200 MeV between 4 August 2008 and 11 March 2009 measured by LAT. The time bin size is 3 days.

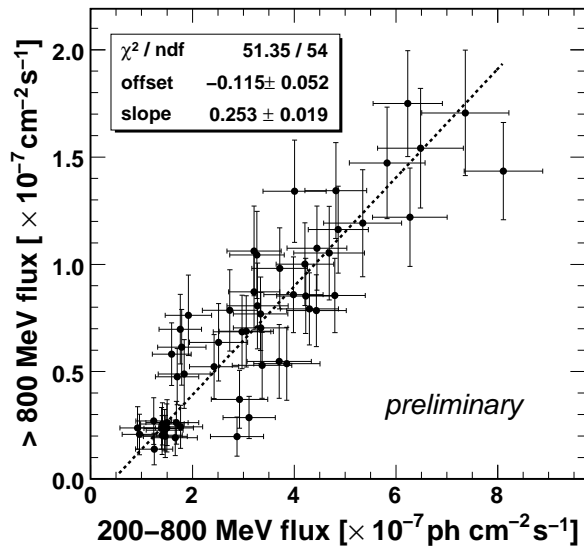


Fig. 3: Flux-flux plot for the energy band 200-800 MeV and for energies above 800 MeV. The time bin size is 3 days. Only points with $TS > 16$ for both bands are plotted. The dotted line represents the best-fitting linear function. The fit parameters are listed in the figure. The plot is well described by the linear function between the soft and hard bands. It suggests that the flux ratio between two bands has no significant dependence on the flux level.

offset of -0.12 ± 0.05 ($\chi^2/\text{ndf} = 51.35/54$). It suggests that the flux ratio between the soft and hard bands has no significant dependence on the flux level. The best-fit line is shown in Figure 3. We also quantified the flux variability during the active period by means of the fractional variability parameter F_{var} in four energy bins: 200-400 MeV, 400-800 MeV, 800-1600 MeV and above 1600 MeV. This is based on the "excess variance" [19], [10] after subtracting the contribution expected from measurement errors ($\sigma_{\text{err},i}$). Using the mean square error

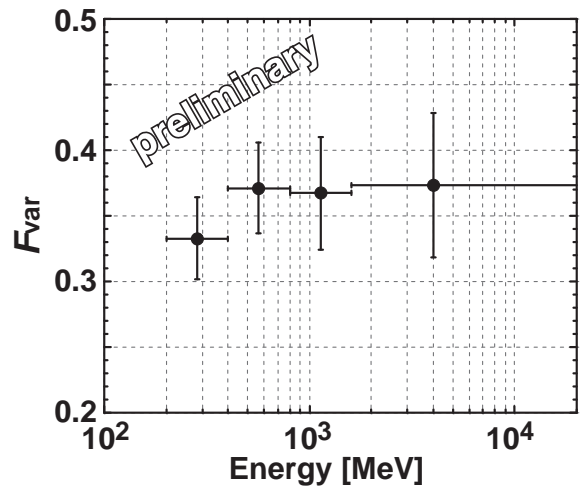


Fig. 4: Fractional variability parameter as derived for four energy bins. Vertical bars denote 1σ uncertainties; horizontal bars indicate the width of each energy bin.

$\langle \sigma_{\text{err},i} \rangle$, F_{var} can be described as [23]

$$F_{\text{var}} = \sqrt{\frac{S^2 - \langle \sigma_{\text{err},i} \rangle^2}{\langle F \rangle^2}} \quad (1)$$

where S is the variance of the flux and $\langle F \rangle$ is the mean value of the flux. The definition of associated error can be found in [23]. Figure 4 shows the derived F_{var} for each energy bin. The plot indicates that the flux variability of the source shows no significant energy dependence in the γ -ray band.

C. Spectra

In this paper, we present the γ -ray spectra in two different states of source activity. The data for the first 1.5 months are used to derive the spectrum in a "low" state while we select the data of 20 days around the day showing the maximum flux (58789 - 58809 MJD) for the "high" state data set.

Assuming a simple power-law model, we obtained photon indices of 2.35 ± 0.07 and 2.29 ± 0.03 for the low and the high states, respectively. We extrapolate

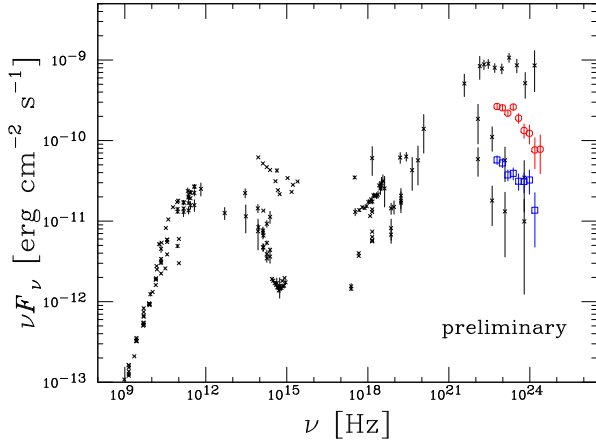


Fig. 5: Spectral energy distribution of 3C 279. Data points of square (blue) and circle (red) refer to the *Fermi*-LAT measured spectra in the low and high states, respectively. Data points of cross (black) are historical data taken from NASA/IPAC Extragalactic Database (NED), and from [13] for the EGRET data. The EGRET data comprise 3 epochs: the maximum [P5b in [13]], a moderate state [P6b] and the lowest state [P2] among the EGRET observations.

the spectra down to 100 MeV for comparison with previous EGRET results. The integrated flux above 100 MeV for the low state corresponds to $F_{E>100\text{MeV}} = (3.7 \pm 0.4) \times 10^{-7}$ photons $\text{cm}^{-2} \text{s}^{-1}$, which is only about a factor of 3 higher than the lowest flux measured by EGRET [16]. The high state spectrum gave $F_{E>100\text{MeV}} = (18.3 \pm 0.6) \times 10^{-7}$ photons $\text{cm}^{-2} \text{s}^{-1}$, which is still about a factor of 3 lower than the historical maximum flux of the source [24], [13]. We also fitted the high state spectrum by a log-parabola model. Compared to the result with the simple power-law model, a likelihood ratio test indicates a hint ($\sim 4\sigma$) of a spectral curvature beyond the simple power-law model. Figure 5 shows an overall spectral energy distribution (SED) of 3C 279 including the measured *Fermi*-LAT spectra as well as some historical data.

More detailed discussions with emission models will be performed together with the data of other energy bands from radio through X-ray.

ACKNOWLEDGMENT

The *Fermi* LAT Collaboration acknowledges support from a number of agencies and institutes for both development and the operation of the LAT as well as scientific data analysis. These include NASA and DOE in the United States, CEA/Irfu and IN2P3/CNRS in France, ASI and INFN in Italy, MEXT, KEK, and JAXA in Japan, and the K. A. Wallenberg Foundation, the Swedish Research Council and the National Space Board in Sweden. Additional support from INAF in Italy for science analysis during the operations phase is also gratefully acknowledged. M. H. is supported by the Japan Society for the Promotion of Science (JSPS) for the Postdoctoral Fellowship for Research Abroad.

REFERENCES

- [1] Albert, J., et al. (MAGIC Collaboration) 2008, *Science*, 320, 1752
- [2] Atwood, W., et al. (*Fermi*-LAT Collaboration) 2009, submitted to *ApJ* (arXiv:0902:1089)
- [3] Blandford, R. D., & Levinson, A. 1995, *ApJ*, 441, 79
- [4] Bloom, S. D., & Marscher, A. P. 1996, *ApJ*, 461, 657
- [5] Chatterjee, R., et al. 2008, *ApJ*, 689, 79
- [6] Collmar, W., et al. 2001, *Gamma 2001: Gamma-Ray Astrophysics*, 587, 271
- [7] Dermer, C. D., Schlickeiser, R., & Mastichiadis, A. 1992, *A&A*, 256, L27
- [8] Dermer, C. D., & Schlickeiser, R. 1993, *ApJ*, 416, 458
- [9] Giuliani, A., et al. 2009, *A&A*, 494, 509
- [10] Edelson R., et al. 2002, *ApJ*, 568, 610
- [11] Hartman, R. C., et al. 1992, *ApJL*, 385, L1
- [12] Hartman, R. C., et al. 1999, *ApJS*, 123, 79
- [13] Hartman, R. C., et al. 2001, *ApJ*, 553, 683
- [14] Hermsen, W., et al. 1993, *A&AS*, 97, 97
- [15] Maraschi, L., Ghisellini, G. & Celotti, A. 1992, *ApJL*, 397, L5
- [16] Maraschi, L., et al. 1994, *ApJL*, 435, L91
- [17] Mattox, J. R., et al. 1996, *ApJ*, 461, 396
- [18] McNaron-Brown, K., et al. 1995, *ApJ*, 451, 575
- [19] Nandra, K., et al. 1997, *ApJ*, 476, 70
- [20] Nandikotkur, G., et al. 2007, *ApJ*, 657, 706
- [21] Sikora, M., Begelman, M. C., & Rees, M. J. 1994, *ApJ*, 421, 153
- [22] Strong, A. W., Moskalenko, I. & Reimer O. 2004, *ApJ*, 613, 962
- [23] Vaughan, S., et al. 2003, *MNRAS*, 345, 1271
- [24] Wehrle, A. E., et al. 1998, *ApJ*, 497, 178